Contents lists available at ScienceDirect

EBioMedicine

Research paper

Alveolar macrophage dysfunction and cytokine storm in the pathogenesis of two severe COVID-19 patients

Chaofu Wang[a,1,*], Jing Xie[a,1], Lei Zhao[b,1], Xiaochun Fei[a,1], Heng Zhang[a,1], Yun Tan[c,1], Xiu Nie[d,1], Luting Zhou[a,1], Zhenhua Liu[e,1], Yong Ren[f], Ling Yuan[f], Yu Zhang[f], Jinsheng Zhang[f], Liwei Liang[f], Xinwei Chen[f], Xin Liu[f], Peng Wang[f], Xiao Han[f], Xiangqin Weng[c], Ying Chen[g], Ting Yu[h], Xinxin Zhang[i], Jun Cai[b,*], Rong Chen[h,*], Zhengli Shi[g,*], Xiuwu Bian[j,*]

[a] Department of Pathology, Ruijin Hospital, Shanghai Jiaotong University School of Medicine, Shanghai, China
[b] Department of Pathology, Shanghai Jiaotong University School of Medicine, Shanghai, China
[c] National Research Center for Translational Research (Shanghai), State Key Laboratory of Medical Genomics, Shanghai Institute of Hematology, Ruijin Hospital, Shanghai Jiaotong University School of Medicine, Shanghai, China
[d] Department of Pathology, Union Hospital, Tongji Medical College, Huazhong University of Science and Technology, Wuhan, Hubei, China
[e] Department of Ultra-sound, Ruijin Hospital, Shanghai Jiaotong University School of Medicine, Shanghai, China
[f] General Hospital of Central Theater Command, PLA
[g] Wuhan Institute of Virology, Chinese Academy of Sciences, Wuhan, China
[h] Department of Pathology, Jin Yin-tan Hospital, Wuhan, China
[i] Research Laboratory of Clinical Virology, Ruijin Hospital and Ruijin Hospital North, Shanghai Jiaotong University School of Medicine, Shanghai, China
[j] Institute of Pathology and Southwest Cancer Center, Southwest Hospital, Third Military Medical University (Army Medical University), Key Laboratory of the Ministry of Education, China

ARTICLE INFO

ABSTRACT

Background: The novel coronavirus pneumonia COVID-19 caused by SARS-CoV-2 infection could lead to a serious of clinical symptoms and severe illness, including acute respiratory distress syndrome (ARDS) and fatal organ failure. We report the fundamental pathological investigation in the lungs and other organs of fatal cases for the mechanistic understanding of severe COVID-19 and the development of specific therapy in these cases.
Methods: The autopsy and pathological investigations of specimens were performed on bodies of two deceased cases with COVID-19. Gross anatomy and histologic investigation by Hematoxylin and eosin (HE) stained were reviewed on each patient. Alcian blue/periodic acid-Schiff (AB-PAS) staining and Masson staining were performed for the examinations of mucus, fibrin and collagen fiber in lung tissues. Immunohistochemical staining were performed on the slides of lung tissues from two patients. Real-time PCR was performed to detect the infection of SARS-CoV-2. Flow cytometry analyses were performed to detect the direct binding of S protein and the expression of ACE2 on the cell surface of macrophages.
Findings: The main pathological features in lungs included extensive impairment of type I alveolar epithelial cells and atypical hyperplasia of type II alveolar cells, with formation of hyaline membrane, focal hemorrhage, exudation and pulmonary edema, and pulmonary consolidation. The mucous plug with fibrinous exudate in the alveoli and the dysfunction of alveolar macrophages were characteristic abnormalities. The type II alveolar epithelial cells and macrophages in alveoli and pulmonary hilum lymphoid tissue were infected by SARS-CoV-2. S protein of SARS-CoV-2 directly bound to the macrophage via the S-protein-ACE2 interaction.
Interpretation: Infection of Alveolar macrophage by SARS-CoV-2 might be drivers of the "cytokine storm", which might result in damages in pulmonary tissues, heart and lung, and leading to the failure of multiple organs .
Funding: Shanghai Guangci Translational Medical Research Development Foundation, Shanghai, China

1. Introduction

The coronavirus disease-19 (COVID-19) caused by SARS-CoV-2 infection can lead to a series of clinical settings from non-symptomatic viral carriers/spreaders to severe illness characterized by acute

* Correspondence authors.
  E-mail addresses: wangchaofu@126.com (C. Wang), caijun@shsmu.edu.cn (J. Cai), crjudy@126.com (R. Chen), zlshi@wh.iov.cn (Z. Shi), bianxiuwu@263.net (X. Bian).
  [1] Contributed equally to this work.

respiratory distress syndrome (ARDS). [1–3] A sizable part of patients with COVID-19 have mild/moderate clinical symptoms at the early stage of infection, but the disease progression may become quite rapid in the later stage with ARDS as the common manifestation and followed by critical multiple organ failure, causing a high mortality rate of 7-10% in the elderly population with non-communicable chronic disease (NCD). [1,2,4] The pathological evidences in the lung of fatal cases are fundamental for the mechanistic understanding and treatment of severe patients with COVID-19. In this study, we investigated the critical pathological changes in the lung of severe COVID-19 patients. We hope this work may contribute in a significant way to the understanding of the mechanisms underlying the phenotype of severe cases in COVID-19 and appropriate development of treatment strategies.

Research in context

Evidence before this study

As the severe acute respiratory syndrome coronavirus 2 (SARS-CoV-2) spreads increasingly worldwide, coronavirus disease 2019 (COVID-19) outbreak has become a common challenge faced by humanity. It can lead to a series of clinical settings from non-symptomatic viral carriers/spreaders to severe illness characterized by acute respiratory distress syndrome (ARDS). So far, up to April 13, 2020, we searched PubMed for articles using "novel coronavirus", "SARS-CoV-2" and "pathology" as keywords, there were two case reports concerning the pathological changes of COVID-19. One case report showed the pathological characteristics of a patient who died from severe infection with severe acute respiratory syndrome coronavirus 2 (SARS-CoV-2) by postmortem biopsies. Another report described the early phase of the lung pathology of COVID-19 pneumonia by lung lobectomies for adenocarcinoma. The former one has limitations for comprehensive observation of organs owing to the biopsy samples, and the latter one only shows the early changes of lungs in patients of COVID-19 with mild symptoms. These reports revealed that the pathological features of COVID-19 greatly resemble those seen in SARS and Middle Eastern respiratory syndrome (MERS) coronavirus infection.

Added value of this study

We performed an anatomical and pathological study in two patients died from COVID-19 and identified the distinct pathological feature of COVID-19. We found mucous plugs in all respiratory tracts, terminal bronchioles and pulmonary alveoli which could aggravate the dysfunction of ventilation and the viral infection of aggregated alveolar macrophages that could result in "cytokine storm" or cytokine release syndrome (CRS).

Implications of all the available evidence

These findings might shed light on the pathogenesis of COVID-19 and potential therapeutic strategies against SARS-CoV-2 among severe patients. The excessive mucus secretion with serous and fibrinous exudation, which could aggravate the dysfunction of ventilation, might be one of the pathogenic mechanisms responsible for the hypoxemia that somehow different from SARS patients. The accumulation of SARS-CoV-2-infected macrophages in the lungs resulted in releasement of cytokines including IL-6 which is considered as one of the drivers in a special clinical setting known as CRS. And these pathological findings supported the notion that anti-IL-6/IL-6R antibody treatment among severe COVID-19 patients might benefit for the blockage of CRS.

---

2. Methods

2.1. Patients and pathological anatomy

The autopsy and pathological investigations of specimens were performed on bodies of two deceased cases with COVID-19 in Wuhan Jin Yin-Tan Hospital, Hubei, China. The diagnosis was established according to clinical symptoms (fever, cough and shortness of breath), RT-PCR testing of SARS-CoV-2 and chest X-ray or computed tomographic (CT) scanning examination (Fig. S1). The severe respiratory and circulatory failure was considered the critical cause of death in the two patients. Informed consent was obtained. This study was approved by the Medical Ethics Committee of the National Health Commission of China. The autopsy procedures were performed in the negative pressure-ventilation P3 Laboratory. We collected adequate pieces of each organ for analysis, special attention was given to the lungs and 38 and 60 pieces were collected respectively. The timelines were 6 hours and 9 hours from death to autopsy.

2.2. Histological, histochemical and immunohistochemical staining

Hematoxylin and eosin (HE) staining of the slides of 10% neutral formaldehyde-fixed, paraffin-embedded tissues was performed and carefully reviewed on each patient. Alcian blue/periodic acid-Schiff (AB-PAS) staining and Masson staining were carried out for the examinations of mucus, fibrin and collagen fiber in lung tissues. Immunohistochemical staining was performed on the slides of lung tissues from two patients. A panel of primary antibodies were used, including the macrophage marker CD68 (Monoclonal mouse anti-human CD68, clone KP1; 1:100; Dako Omnis, Agilent); T-lymphocyte marker CD3 (Monoclonal rabbit anti-human CD3, clone SP7; ready-to-use; Dako Omnis, Agilent), CD4 (Monoclonal mouse anti-human CD4, clone 4B12; ready-to-use; Dako Omnis, Agilent) and CD8 (Monoclonal mouse anti-human CD8, clone C8/144B; ready-to-use); B-lymphocyte markers CD20 (Monoclonal mouse anti-human CD20cy, clone L26; ready-to-use); natural killer cell/T cell (NK/T cell) marker CD56 (Monoclonal mouse anti-human CD56, clone 123C3; ready-to-use), and the markers of Programmed Cell Death-1 (PD-1 Monoclonal mouse anti-human PD-1, clone UMAB199; ready-to-use) and Programmed Cell Death-Ligand 1 (PD-L1 Monoclonal mouse anti-human PD-L1, clone 22C3; ready-to-use). Antibodies specific for chemokine and inflammatory cytokines were also used, including interleukin 6 (polyclonal rabbit anti-IL-6 human; 1:250; abcam), interleukin 10 (IL-10, polyclonal rabbit anti-human IL-10; 1:300; abcam) and tumor necrosis factor α (TNFα, polyclonal rabbit anti-human TNFα; 1:80; abcam). In addition, ACE2 protein was revealed using a mouse monoclonal anti-human ACE2 antibody (clone 1G4; 1:160; ORIGENE) while the detection of SARS-CoV-2 was performed using the antibody against SARS-CoV-2 Rp3 N-protein (Rp3-NP) (1:100; the Rp3-NP antibody was provided by Prof. Zheng-Li Shi, Wuhan Institute of Virology, Chinese Academy of Sciences).

2.3. Real-time PCR

Total RNAs were extracted from paraffin-embedded lung and pulmonary hilum lymph nodes tissues, with AmoyDx® FFPE RNA Kit (ADx-FF04, Amoydiagnostics, Xiamen, China) according to manufactures' instructions. The SARS-CoV-2 was detected by real-time RT-PCR with Taqman probes against the E gene, N gene and RdRp gene of SARS-CoV-2 according to manufactures' instruction of the 2019-nCoV nuclear acid detection kit (Z-RR-0479-02-25, Liferiver, Shanghai, China).

2.4. Flow cytometry analysis

2.4.1. Preparation of cells in lung tissues

The normal lung tissues used for preparation of cell suspension subject to flow cytometry analysis were those adjacent to lung tumors obtained from surgical operation. Informed consent was obtained. The normal lung tissues were cut into slices and digested with Type IV Collagenase (#C5138, Sigma) in DMEM (Gibico) supplemented with 10% fetal bovine serum (Gibico) in 37°C for 25 minutes. The indigestible tissues and debris were filtered with a 70 μm cell strainer (#352350, BD Falcon) and the cells were washed twice with PBS. The red blood cells were removed according to manufactures' instructions of Red Blood Cell Lysis Buffer (#40401ES60, Yeasen, China).

2.4.2. Preparation of cells in peripheral blood

The white blood cells were obtained from six health donors according to manufactures' instructions of Red Blood Cell Lysis Buffer (#40401ES60, Yeasen, China). After the removal of the red blood cells, white blood cells were washed twice with PBS.

2.4.3. Antibody and S protein of SARS-CoV-2 labeling and detection

Cells were firstly incubated with Fc blocker (Human BD Fc Block^{TM}, #564219, BD Biosciences). Then they were washed and used incubation for reagents in two different settings: purified SARS-CoV-2 (2019-nCoV) Spike Protein (#40591-V02H, Sino Biological, China), whereas the other with rabbit anti-human ACE2 antibodies (#21115-1-AP, Proteintech, China) in DMEM (Gibico) supplemented with 10% FBS (Gibico) for 30 minutes at room temperature, followed by goat anti-rabbit IgG (Alexa Fluor 546 Goat anti-Rabbit IgG (H+L) polyclonal antibody, ThermoFisher) as secondary antibodies according to manufactures' instructions. Subsequently, cells treated with the above mentioned reagents in two experimental settings were respectively labeled simultaneously by antibodies against human CD3 (APC mouse anti-human CD3 monoclonal antibody, clone HIT3a, BD Bioscience),

CD14 (FITC mouse anti-human CD14 monoclonal antibody, clone RMO52, Beckman Coulter), CD68 (PE/Cy7 mouse anti-human CD68 monoclonal antibody, clone Y1/82A, Biolegend) and human IgG (PE anti-human IgG Fc, clone M1310G05, Biolegend). BD LSRFortessa^{TM} X-20 was used for flow cytometry analysis.

3. Results

The two deceased COVID-19 patients, with the diagnosis confirmed by reverse transcriptase-polymerase chain reaction (RT-PCR) for SARS-CoV-2, were a 53 years old female (Patient No 1) and a 62 years old male (Patient No 2) (Table 1). Both had fever, cough and shortness of breath and received anti-viral treatment with Arbidol and Peramivir respectively. Patient No 2 also received Methylprednisolone therapy (Table 1). Unfortunately, both patients progressed into acute respiratory distress syndrome (ARDS) due to severe pulmonary lesions, as confirmed by chest X-ray or computer-assisted tomography (CT) examinations (Fig. S1). Both patients had significantly decreased lymphocytes with elevated serum IL-6 and C reactive protein (CRP) levels (Table S1), typical worse prognostic indicators in patients with critical disease described in several recent reports. [1−3] The female case had also co-morbidities of type 2 diabetes and essential hypertension. Finally, both cases died of respiratory failure and heart failure.

The pathological investigations of severe patients are pivotal for the understanding of pathogenesis of COVID-19 and assessment of clinical treatments. Special attention was given to the abnormalities in lungs, which are the main damaged organ in severe COVID-19 patients. The gross anatomy of the lungs showed moderate bilateral pleural effusion and fibrotic pleural adhesion in the two patients. The hepatization of pulmonary tissues was observed on the cut-surface of the collapsed and consolidated lungs. The microscopic manifestation of the lung injury was consistent with diffuse alveolar damage (DAD). Alveolar cavities were filled with a large number of macrophages with scattered neutrophils and lymphocytes (Fig. 1a). The massive

Table 1
Clinical features and treatments of two fatal cases of COVID-19/SARS-CoV-2

	Patient no 1	Patient no 2
Gender	Female	Male
Age (years)	53	62
Days from appearance of symptoms to hospital admission (days)	20	13
Duration of hospitalization (days)	8	10
RT-PCR for SARS-CoV-2 (pharyngeal swab)	Positive	Positive
Symptoms (fever, cough, shortness of breath)	Yes	Yes
Co-morbidities	Type 2 diabetes and Hypertension	No
Secondary pulmonary infection	No	No
Shock	No	No
Arrhythmia	No	No
Renal failure	Yes	No
Antiviral therapy	Arbidol (Dpoi 22-28)	Peramivir (Dpoi 11-13)
Steroids therapy	No	Methylprednisolone 80mg QD iv. dri (Dpoi 14)
Ventilator support	Non-invasive mechanical Ventilation (CPAP/PSV) FiO$_2$ 90%, PEEP 13cmH$_2$O PS 20cmH$_2$O, R15bpm	Nasal cannular oxygenation and mask oxygen inhalation
Oxygen saturation	99% (Dpoi 21) 99% (Dpoi 23) 100% (Dpoi 24) 100% (Dpoi 27) 80% (Dpoi 28)	78% (Dpoi 14) 95% (Dpoi 16) 92% (Dpoi 18) 72% (Dpoi 19) 89% (Dpoi 20) 98% (Dpoi 22) 98% (Dpoi 23)
Cause of death	Respiratory failure Heart failure	Respiratory failure Heart failure

Dpoi: day post onset of illness
The patient No 1 maintained blood oxygen saturation under the ventilator support, the blood oxygen saturation dropped sharply at 28 days post onset of illness, and died after ineffective rescue.
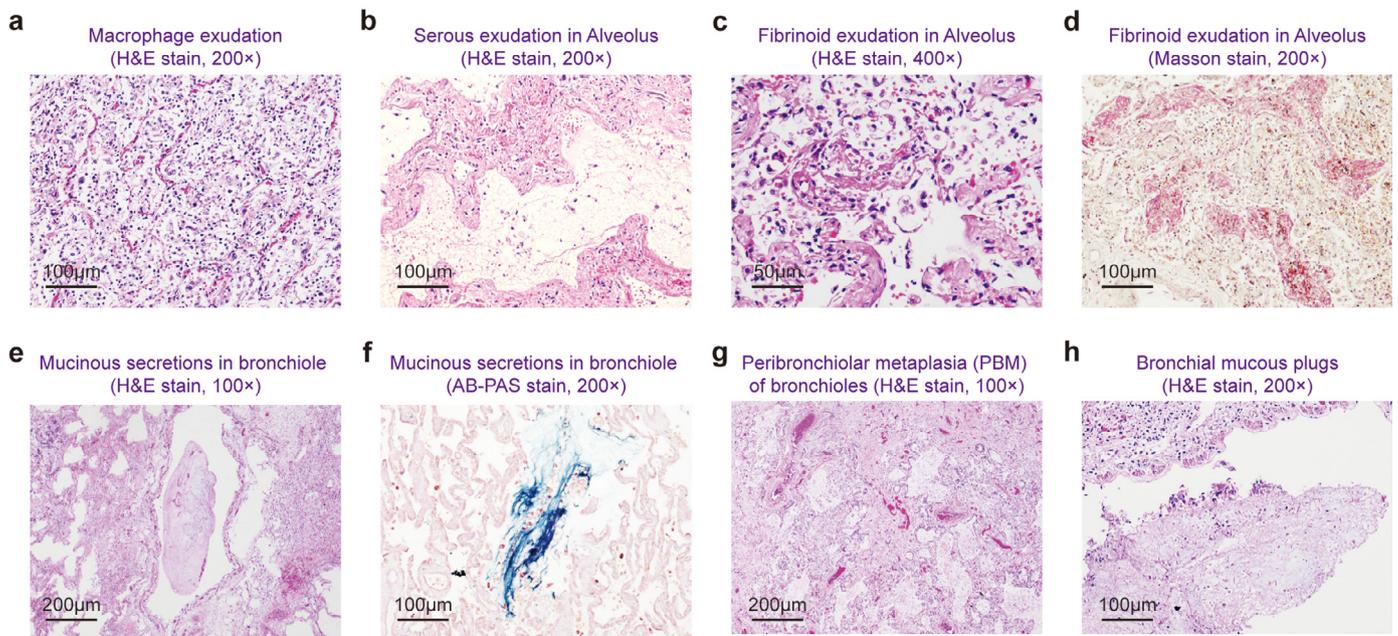
Fig. 1. Extensive exudate and mucinous secretion. (a) A large number of macrophages in alveolar cavities (H&E stain, 200 ×). (b-d) Serous (B, H&E stain, 200 ×) and fibrinoid (c, H&E stain, 400 ×, d, Masson stain, 200 ×) exudation. Mucinous secretions in bronchioles (e, H&E stain, 100 ×) with blue staining by AB-PAS stain (f, 200 ×). Peribronchiolar metaplasia (PBM) of bronchioles and terminal bronchioles (g, H&E stain, 100 ×) as well as bronchial mucous plugs formation (h, H&E stain, 200 ×) are visible.

serous (Fig. 1b) and fibrinoid exudate in the alveolar spaces were shown by the Masson staining (Figs. 1c−d). The acidic mucopolysaccharides from a large amount of mucinous secretion were observed by the Alcian blue-periodic acid-Schiff (AB-PAS) staining in the bronchi and bronchioles, terminal bronchioles and pulmonary alveoli (Figs. 1e−f). A lot of mucus in the distal respiratory tract lined by mucous cells was shown, reminiscent of the morphology of mucoid adenocarcinoma (Fig. 1g). The peribronchiolar metaplasia (PBM) with interstitial fibrous hyperplasia but without invasive growth of atypical cells was observed. The bronchial plug combined with epithelial detachment was visible (Fig. 1h).

The hyaline membranes and widened alveolar walls with collagen fibers proliferation and lymphocyte infiltration were observed in alveoli occasionally (Figs. S2a-b). Focal or patchy hemorrhage with fibrinous exudate was seen in the alveolar cavities and interstitial tissues (Figs. S2c-d). The broken alveolar walls flushed by huge hemorrhagic effusion formed the "blood lake". The endothelial cells of small pulmonary arteries were swollen and shed (Fig. S2e). Mixed thrombi were present in small veins (Fig. S2f).

Intensive sloughing of bronchiole and alveolar epithelial cells was remarkable (Figs. 2a−b) while abundant swollen and degenerated alveolar cells desquamated in the alveoli (Figs. 2c−d). Patchy type II pneumocytes proliferated with atypical changes, including enlarged nuclei, clearing of nuclear chromatin, prominent nucleoli and inclusion bodies (Figs. 2e−f). The proliferation of type alveolar epithelial cells resembled the morphological changes of atypical adenomatous hyperplasia, in situ adenocarcinomas, or even invasive adenocarcinoma. Thickened alveolar walls and widened interstitial tissues were accompanied by lymphocyte infiltration and fibroblast proliferation (Figs. 2g−h).

Notably, the alveolar macrophages significantly increased and filled in a part of the alveolar cavities with scattered neutrophils and lymphocytes. CD68, one of the scavenger receptors and a well-documented specific marker of macrophages, [5] was highly expressed in alveolar macrophages. These CD68 positive macrophages were presented in diverse forms, including aggregation in small clusters (Figs. 3a−b), diffused distribution (Fig. 3c), single cell exhibiting intracytoplasmic phagocytosis, spherical acidophilic hyaline bodies or hemophagocytic phenomenon (Figs. 3d−e), and multinucleated

giant cells (Fig. 3f). Furthermore, using immunohistochemistry approach, we examined several chemokine and inflammatory cytokines secreted by alveolar macrophages including IL-6, IL-10 and TNFα with specific antibodies. IL-6 and TNFα were moderately expressed in macrophages (Figs. 3g−i), while the expression of IL-10 was strong (Fig. 3h). Besides, extensive and strong expression of Programmed Death-Ligand 1 (PD-L1) by alveolar macrophages was observed (Fig. 3j).

Of particular note, we found the expression of ACE2, a well-established receptor for both SARS-CoV and SARS-CoV-2, by hyperplastic type II alveolar epithelial cells and alveolar macrophages (Fig. 4a). Macrophages in the cortical sinuses of pulmonary hilum lymph nodes were also shown to express ACE2 (Figs. 4d and 4g). Moreover, type II alveolar epithelial cells and macrophages in alveoli and pulmonary hilum lymphoid tissue were infected by SARS-CoV-2, as revealed by immunohistochemistry using Rp3-NP specific antibodies (Figs. 4b, e and h). This result was further confirmed by real-time RT-PCR detection (Table S2).

Next, the distribution of lymphocytes in the pulmonary tissues was examined. A recent report had described the substantially reduced peripheral T cells and lymphocytes infiltration in lung tssue [6]. Contrarily to the situation of macrophages, the degree of lymphocytic infiltration was much inferior, although some focal infiltrations of lymphocytes were present (Fig. S3a). CD20-positive B lymphocytes (Fig. S3b) accounted for a large majority of the lymphocytes whereas a few CD3-positive T lymphocytes (Fig. S3c) made up a small proportion including CD4-strong positive for helper T cells and CD8-positive for cytotoxic T cells (Figs. S3d-e). Among the inflammatory infiltrating cells, no CD56-positive NK/T cells (Fig. S3f) were detected. Neither Programed cell death protein-1 (PD-1) nor PD-L1 proteins were shown on the surface of lymphocytes (Figs. S3g-h). No obvious viral infection was found in the lymphocytes and mesenchymal cells by using Rp3-NP antibody in immunohistochemistry staining (Fig. S3i).

To further address the topic that monocytes/macrophages could be the direct target cells of SARS-CoV-2, cell suspension from the normal lungs were incubated respectively with purified S proteins or anti-human ACE2 antibodies, followed by an incubation with directly labeled antibodies against cell surface markers CD14 (covering several blood cell lineages, but with strong binding with monocytes),
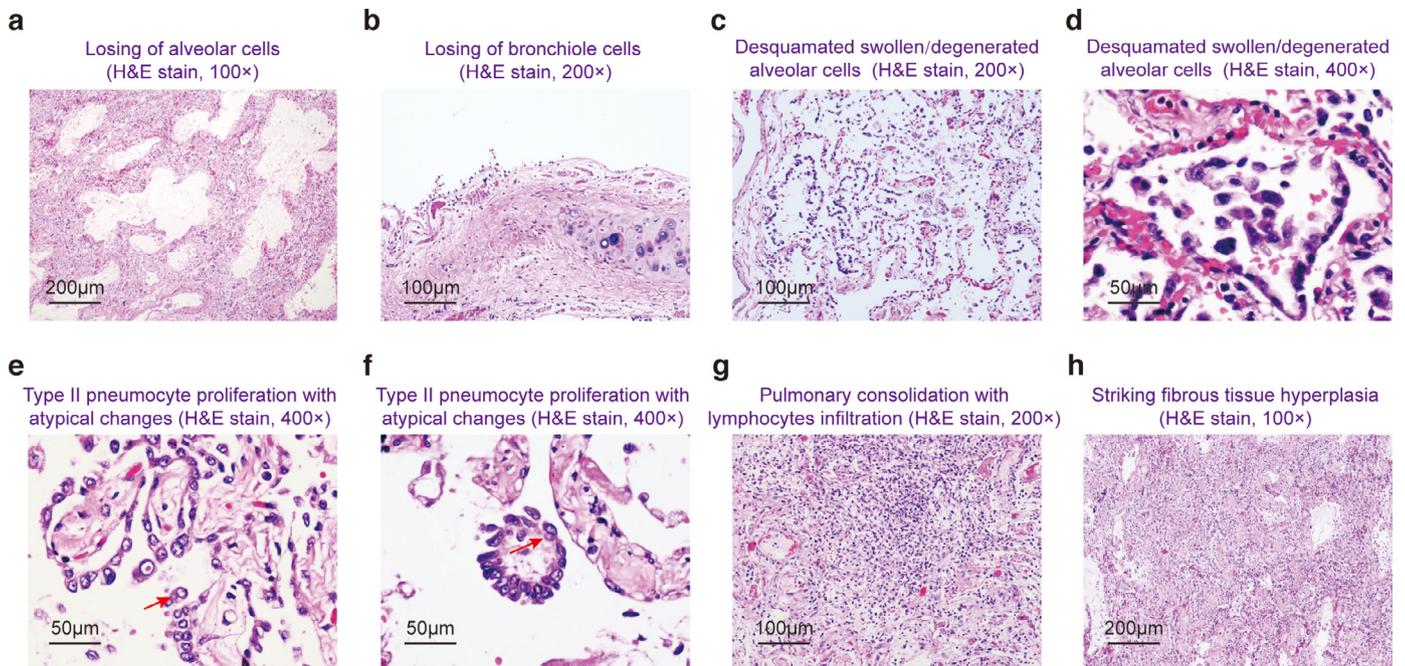
Fig. 2. Damage of respiratory tracts and reparative changes. (a-b) Intensive sloughing of alveolar (a, H&E stain, 100 ×) and bronchiole (b, H&E stain, 200 ×) epithelial cells. (c-f) Desquamated swollen and degenerated alveolar cells in alveoli (H&E stain, c, 200 × and d, 400 ×); type II pneumocyte proliferation with atypical changes (e and f, H&E stain, 400 ×): enlarged nuclei, clearing of nuclear chromatin and prominent nucleoli. Inclusion bodies are indicated by arrow. (g-h) Pulmonary consolidation with infiltration of lymphocytes (g, H&E stain, 200 ×) and striking fibrous tissue hyperplasia (h, H&E stain, 100 ×).
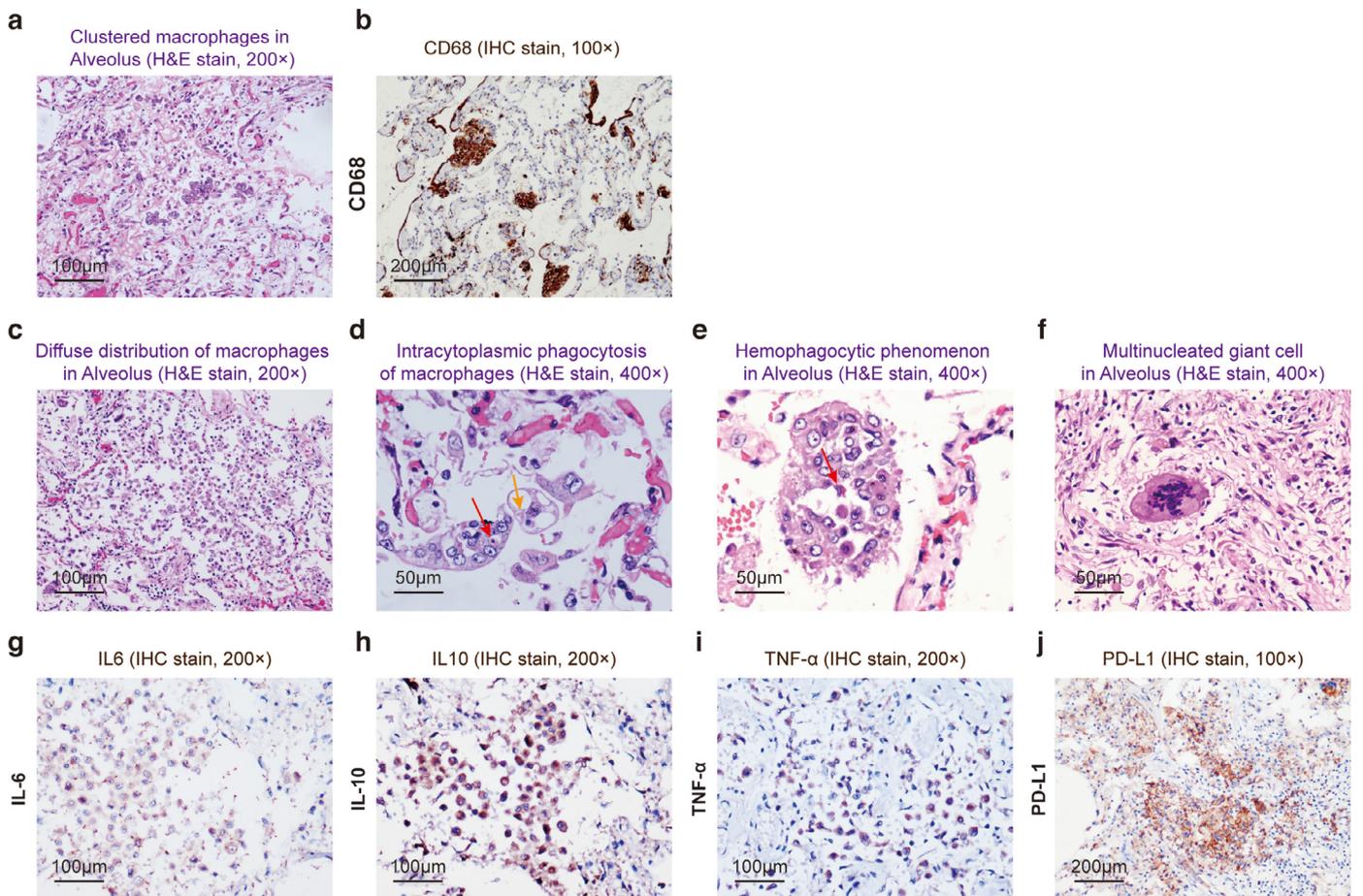
Fig. 3. Aggregated alveolar macrophages. (a-f) A large number of mononuclear and multinucleate macrophages in alveoli in varied forms: in clusters (a, H&E stain, 200 ×) and immunohistochemistry staining of CD68 (b); Diffuse distribution (c, H&E stain, 200 ×); Intracytoplasmic phagocytosis (d, H&E stain, 400 ×, indicated by red arrow) and Spherical acidophilic hyaline degeneration bodies (indicated by orange arrow); Hemophagocytic phenomenon (e, H&E stain, 400 × indicated by red arrow) and multinucleated giant cell (f, H&E stain, 400 ×). (g-j) Expression of chemokine and inflammatory cytokines: IL-6 (g, 200 ×), IL-10 (h,200 ×), TNFα (i, 200 ×) and extensive expression of PD-L1 (j, 100 ×)
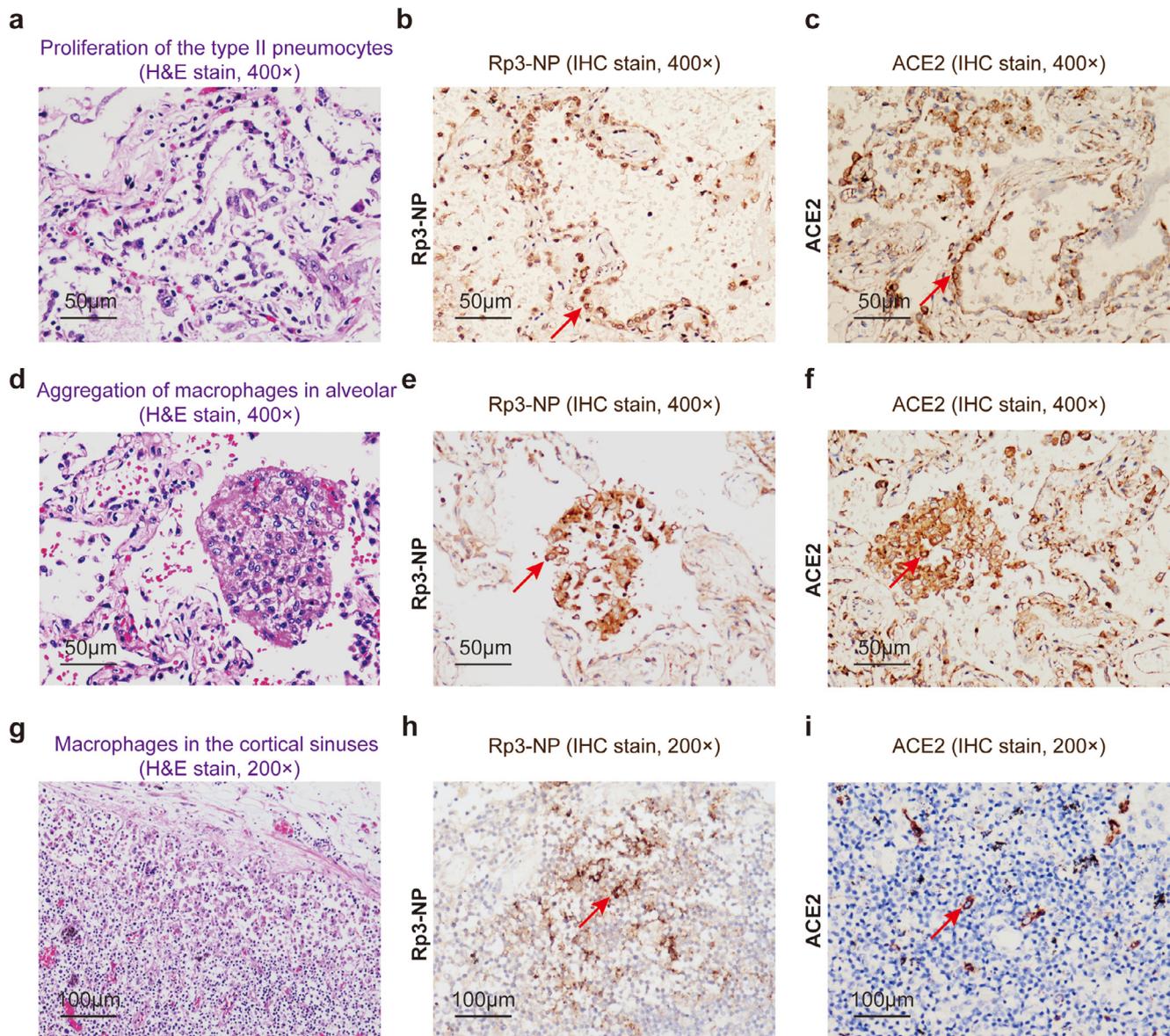
Fig. 4. COVID-19-infected cells in lung and pulmonary hilum lymph nodes. Proliferation of the type II pneumocytes by H&E stain (a, 400 ×) and expression of Rp3-NP by immuno-histochemistry in type II pneumocytes (b, 400 ×, arrow); Membrane positive of ACE2 expression in type II pneumocytes and macrophages respectively (c, 400 ×, arrow and f, 400 ×, arrow); Aggregation of macrophages in alveolar by H&E stain (d, 400 ×) and expression of Rp3-NP of SARS-CoV-2 (e, 400 ×, arrow); Macrophages in the cortical sinuses of pulmonary hilum lymph nodes (g, 200 ×), expression of Rp3-NP of SARS-CoV-2 (h, 200 ×, arrow) and ACE2 (i, 200 ×, arrow).

CD3 (T cells) and CD68 (specific marker of macrophages). The labeled cells were then subject to flow cytometry analysis. Of note, there were high levels of S protein binding on the lung macrophages (Fig. 5a). Furthermore, ACE2 was also highly expressed on the surface of the lung macrophages (Fig. 5b), suggesting SARS-CoV-2 could enter into the alveolar macrophage via the interaction between S protein and ACE2 receptor [7]. Since the monocytes/macrophages in the peripheral blood are well established as sources of tissue macrophages, we tested S protein binding to white blood cell (WBC) samples from six healthy donors. The results of flow cytometry analysis showed that the S protein interacted with CD68-expressing monocytes/macrophages but not with T lymphocytes (Fig. 5c). When the expression of ACE2 was examined on the surface of blood monocytes/macrophages, an expression pattern similar to that of S protein was observed (Fig. 5d).

We carefully examined, in the two deceased patients, the heart and kidney which were often found with damaged functions in SARS-CoV-2 infected people. No obvious gross abnormalities were observed. Nevertheless, microscopical abnormalities were found in both organs. Multifocal myocardial degeneration was present in the heart, together with myocardial atrophy and interstitial fibrous tissue hyperplasia (Figs. S4a-b). A few CD20-positive B cells and CD3-positive T cells were scattered in the heart (Figs. S4c-d). In the kidneys, normal renal structures were retained. Nonetheless, the fibrotic glomeruli and edematous tubular epitheliums were focally present with a small amount of infiltrating B and T lymphocytes (Figs. S4e-h). It is worth noting that no obvious viral infection was found in parenchymal cells in both heart and kidney using immunohistochemistry with antibodies against Rp3-NP.

4. Discussion

Overall speaking, pathological findings in pulmonary tissues of COVID-19 shared similarities to those in SARS outbreak of 2003.

In both diseases, extensive damage of type I alveolar epithelial cells and atypical hyperplasia of type II alveolar cells were detected,
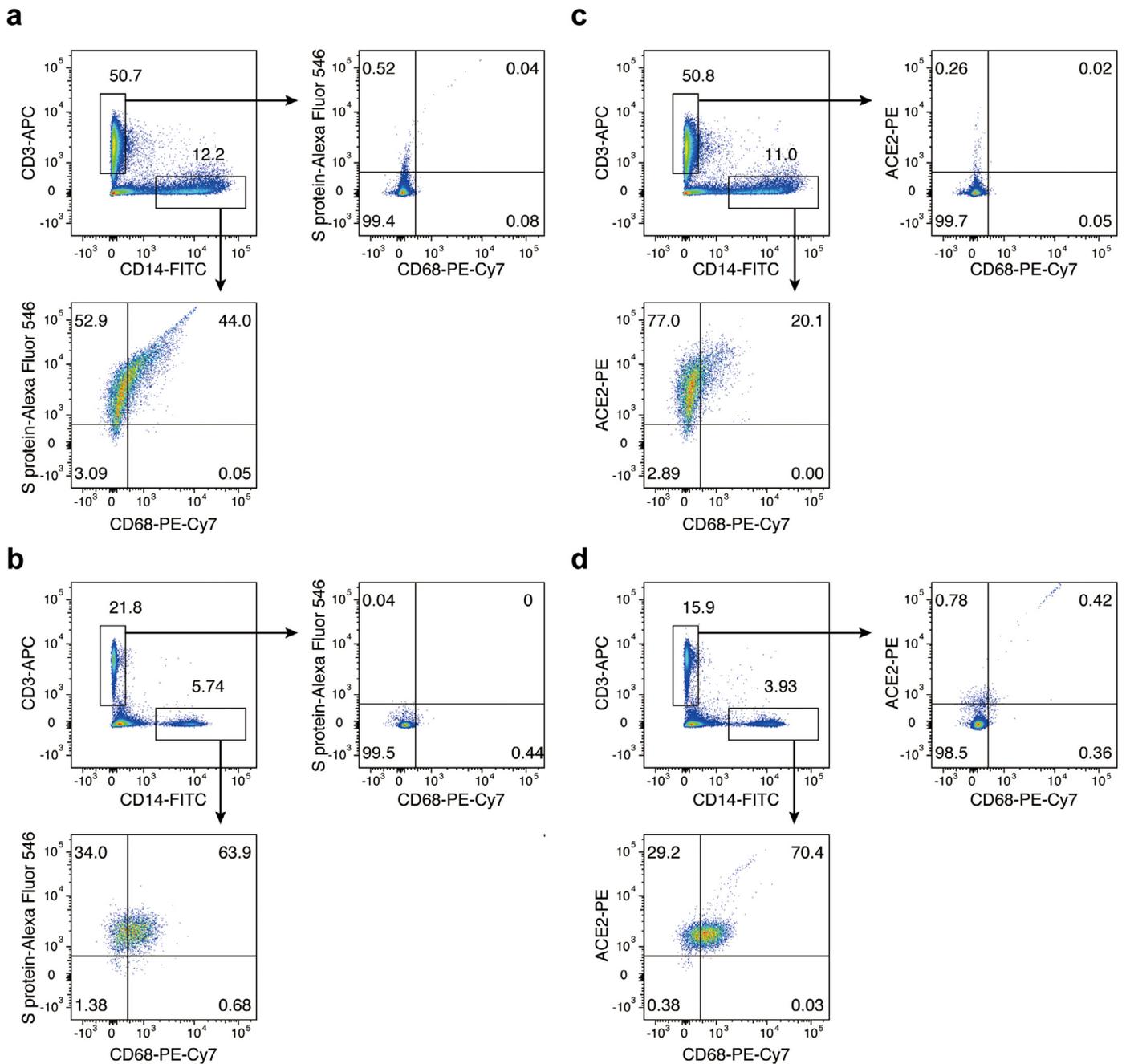
Fig. 5. SARS-CoV-2 Spike protein interaction with CD68 macrophage. (a-b) Flow cytometry analysis showing the distribution of S protein bound immune cells in lung tissues (a) and peripheral blood. (b) CD14 markers were used for labeling monocytes/ macrophages while CD3 for T cells. (c-d) Flow cytometry analysis showing the expression of ACE2 on the surface of monocytes/macrophages, but not of T cells in lung tissues (c) and peripheral blood (d).

with formation of hyaline membrane, focal hemorrhage, exudation and pulmonary edema, and pulmonary consolidation. The sloughing of epithelium, also a classic and common appearance of expected postmortem tissue changes, were extensively present in our cases and a recent report [8]. It is one of common manifestations in the diffuse alveolar damage (DAD) that existed in acute respiratory distress syndrome (ARDS) not only in COVID19 but also in SARS and MERS. Meanwhile, infiltration of macrophages, lymphocytes and plasma cells, as well as endothelial injury and thrombosis in small vessels and micro-vascular structures in the lungs were obvious in the two diseases. Thus, like SARS-CoV, SARS-CoV-2 was capable of triggering the pathogenesis and resulting in severe dysfunction of ventilation and gas exchange obstruction in patients. [9−13] Though the endothelial injury and thrombosis were not common in our cases,

resent studied showed the high incidence of thromboembolic events in segmental/subsegmental pulmonary arterial vessels [14], pulmonary embolism and deep venous thrombosis [15], and microvascular thrombosis [16], suggested coagulopathy in severe COVID-19 infection patients.

However, the pathology of lungs in COVID-19 also exhibited unique features as compared to SARS. For example, in the previous autopsy study on SARS, the hyaline membranes in alveoli were reported, [9] which constituted the major anatomical abnormalities leading to gas exchange obstruction, whereas the hyaline membranes in alveoli were uncommon in our observations, which was in accordance with a recent report [17]. In COVID-19, we found mucous plugs in all respiratory tracts, terminal bronchioles and pulmonary alveoli, which was not described in SARS. [9,11−13,18,19] One patient

received 3-days non-invasive ventilator treatment while the other had nasal cannular oxygenation and mask oxygen inhalation instead of ventilator treatment (Table 1), indicating the mucous plugs obstruction was not caused by the ventilator-induced lung injury (VILI). Another unique feature of COVID-19 was the excessive mucus secretion with serous and fibrinous exudation, which could aggravate the dysfunction of ventilation. Therefore, the pathogenic mechanisms responsible for the hypoxemia could be somehow different between COVID-19 and SARS patients. We assumed these lesions could play a part in the sputum suction failure in very severe COVID-19 patients. In addition, the differences between COVID-19 and SARS could be found at the level of immune cell involvement. It was reported that SARS-CoV could occasionally be identified in the alveolar macrophages. [10] In the case of COVID-19, the viral infection of aggregated alveolar macrophages was obvious from early phase to the late stage, according to our study and the results in recent reports of pulmonary pathology [17,20]. These observations suggest the alveolar macrophages might be crucial in the pathological changes in patients with critical disease manifestation, in that the aggregation and activation of these cells could result in "cytokine storm" or cytokine release syndrome (CRS). The spectacular infiltration and activation of alveolar macrophages in COVID-19 might represent the shift of classically activated phenotype (M1) to alternatively activated phenotype (M2) of these cells, whereas this shift, particularly in the case of antibody-dependent enhancement (ADE), could contribute to the inflammatory injuries and fibrosis of respiratory tracts. [21] And the specific subsets of macrophages should be identified in future studies.

To further address the significance of accumulation of macrophages in lungs and to explore the potential function of monocytes/macrophages in response to SARS-CoV-2, we examined the possible interaction between spike (S) protein of SARS-CoV-2 and ACE2 receptor on the surface of immune cells isolated from pulmonary tissues. These findings were in support of a direct viral entry into the monocytes/macrophages and highlighted the role of the aberrantly activated macrophages as host cells of SARS-CoV-2 in COVID-19 disease mechanism.

In agreement with abnormal activation of macrophages, an elevated serum IL-6 was observed in the two cases in this study, consistent to recent reports by other groups [3]. Release of cytokines including IL-6 by macrophages has been considered as one of the drivers in a special clinical setting known as CRS in hemophagocytic lymphohistocytosis (HLH) or macrophage activation syndrome (MAS). [22,23] The blockage of CRS using anti-IL-6 or IL-6R antibody, such as Tocilizumab, has already been used in the treatment of MAS or HLH. Recently, the Tocilizumab therapy was recommended in the Guideline of Diagnosis and Treatment of COVID-19 (version 7) by the National Health Commission in China to control the CRS. While potential benefits of this treatment still require definite evidence, our pathological findings tend to support the clinical practice of the anti-IL-6/IL-6R antibody treatment among severe COVID-19 patients in order to inhibit the vicious cycle of alveolar macrophage activation and inflammatory injuries. On the other hand, the use of anti-viral effect of convalescent plasma from recovered patients has been shown to be effective in the treatment of severe cases of COVID-19. [24]

It is well known that elderly patients with NCD such as diabetes, cardiovascular disease and hypertension are vulnerable to COVID-19. We carefully examined, in the two deceased patients, the heart and kidney which were often found with damaged functions in SARS-CoV-2 infected people. No obvious gross abnormalities were observed. Nevertheless, microscopical abnormalities were found in both organs. It is worth noting that no obvious viral infection was found in parenchymal cells in both heart and kidney using immunohistochemistry with antibodies against Rp3-NP

Finally, some issues remain to be addressed in future studies. First, the precise molecular and cellular mechanisms underlying the infection of alveolar macrophages by SARS-CoV-2 should be unfolded so that a deeper understanding of the persistent viral infection and inadequate immune reaction in severe/critical cases of COVID-19 can be obtained. These studies may accelerate and refine drug and vaccine design targeting vulnerabilities of viral entry and proliferation in affected cells/tissues. Second, in the two cases studied here and in some other recent reports, there is a remarkable reduction of both CD4 and CD8 cells in the peripheral blood in COVID-19 patients. A graded decrease of T cells was found with increased clinical severity. Intriguingly, we recently observed a negative correlation between the extent of T lymphocytopenia and increased IL-6 and Il-8 levels in the serum. The causal relationship between these phenomena should be addressed. Third, in this study, no ACE2-expression was found on the surface of T cells, which might be considered as an argument for the absence of direct toxic effect of SARS-CoV-2 on distinct T cell populations. However, the observation of only a small number of T lymphocytes in the inflammatory lung tissues at late disease stage might not reflect the status of T cell infiltration at relatively early phase of COVID-19. The possibility that the reduction of peripheral blood T cells result from a tremendous infiltration of these cells into lung tissues in early response to the effect of cytokines and a subsequent apoptosis of these cells cannot be ruled out. The study on detailed mechanism of T cell depletion in severe COVID-19 over the whole disease process should be conducted among patients or in experimental animal models.

Declaration of Competing Interest

The authors declare no competing interests.

Author contributions

C. W., J. X. and R. C. conceived and designed the study, L. Z., X. F., H. Z., Y.T., X.N., X. W., Z. L., Y. R., L. Y., Y. Z., J. Z., L. L., X. C., X. L., P. W., X. H., Y. C., T. Y. Z. S., performed experiments and data analysis. J. C., X. Z. and X. B. contributed to discussion and revision of the manuscript.

Supplementary materials

Supplementary material associated with this article can be found in the online version at https://doi.org/10.1016/j.ebiom.2020.102833.

References

1 Huang C, Wang Y, Li X, et al. Clinical features of patients infected with 2019 novel coronavirus in Wuhan, China. Lancet 2020;395(10223):497–506.

2 Guan WJ, Ni ZY, Hu Y, et al. Clinical characteristics of coronavirus disease 2019 in China. N Engl J Med 2020.

3 Zhou F, Yu T, Du R, et al. Clinical course and risk factors for mortality of adult inpatients with COVID-19 in Wuhan, China: a retrospective cohort study. Lancet 2020;395(10229):1054–62.

4 Chen N, Zhou M, Dong X, et al. Epidemiological and clinical characteristics of 99 cases of 2019 novel coronavirus pneumonia in Wuhan, China: a descriptive study. Lancet 2020;395(10223):507–13.

5 Kunisch E, Fuhrmann R, Roth A, Winter R, Lungershausen W, Kinne RW. Macrophage specificity of three anti-CD68 monoclonal antibodies (KP1, EBM11, and PGM1) widely used for immunohistochemistry and flow cytometry. Ann Rheum Dis 2004;63(7):774–84.

6 Xu Z, Shi L, Wang Y, et al. Pathological findings of COVID-19 associated with acute respiratory distress syndrome. Lancet Respir Med 2020;8(4):420–2.

7 Zhou P, Yang XL, Wang XG, et al. A pneumonia outbreak associated with a new coronavirus of probable bat origin. Nature 2020;579(7798):270–3.

8 Yan L, Mir M, Sanchez P, et al. Autopsy report with clinical pathological correlation. Arch Pathol Lab Med 2020.

9 Peiris JS, Chu CM, Cheng VC, et al. Clinical progression and viral load in a community outbreak of coronavirus-associated SARS pneumonia: a prospective study. Lancet 2003;361(9371):1767–72.

10 Ksiazek TG, Erdman D, Goldsmith CS, et al. A novel coronavirus associated with severe acute respiratory syndrome. N Engl J Med 2003;348(20):1953–66.

11 van der Hoek L, Pyrc K, Jebbink MF, et al. Identification of a new human coronavirus. Nat Med 2004;10(4):368–73.

12 Ding Y, Wang H, Shen H, et al. The clinical pathology of severe acute respiratory syndrome (SARS): a report from China. J Pathol 2003;200(3):282–9.

13 Nicholls JM, Poon LL, Lee KC, et al. Lung pathology of fatal severe acute respiratory syndrome. Lancet 2003;361(9371):1773–8.

14 Lax SF, Skok K, Zechner P, et al. Pulmonary arterial thrombosis in COVID-19 with fatal outcome: results from a prospective, single-center, clinicopathologic case series. Ann Intern Med 2020.

15 Wichmann D, Sperhake JP, Lutgehetmann M, et al. Autopsy findings and venous thromboembolism in patients with COVID-19. Ann Intern Med 2020.

16 Magro C, Mulvey JJ, Berlin D, et al. Complement associated microvascular injury and thrombosis in the pathogenesis of severe COVID-19 infection: a report of five cases. Transl Res 2020.

17 Zeng Z, Xu L, Xie XY, et al. Pulmonary pathology of early phase COVID-19 pneumonia in a patient with a benign lung lesion. Histopathology 2020.

18 Lee N, Hui D, Wu A, et al. A major outbreak of severe acute respiratory syndrome in Hong Kong. N Engl J Med 2003;348(20):1986–94.

19 Drosten C, Gunther S, Preiser W, et al. Identification of a novel coronavirus in patients with severe acute respiratory syndrome. N Engl J Med 2003;348(20):1967–76.

20 Tian S, Hu W, Niu L, Liu H, Xu H, Xiao SY. Pulmonary pathology of early-phase 2019 novel coronavirus (COVID-19) pneumonia in two patients with lung cancer. J Thorac Oncol 2020.

21 Hussell T, Bell TJ. Alveolar macrophages: plasticity in a tissue-specific context. Nat Rev Immunol 2014;14(2):81–93.

22 Billiau AD, Roskams T, Van Damme-Lombaerts R, Matthys P, Wouters C. Macrophage activation syndrome: characteristic findings on liver biopsy illustrating the key role of activated, IFN-gamma-producing lymphocytes and IL-6- and TNF-alpha-producing macrophages. Blood 2005;105(4):1648–51.

23 Cheung CY, Poon LL, Ng IH, et al. Cytokine responses in severe acute respiratory syndrome coronavirus-infected macrophages in vitro: possible relevance to pathogenesis. J Virol 2005;79(12):7819–26.

24 Duan K, Liu B, Li C, et al. Effectiveness of convalescent plasma therapy in severe COVID-19 patients. Proc Natl Acad Sci USA 2020.